# X-ray lithography, from 500 to 30 nm: X-ray nanolithography

by Henry I. Smith M. L. Schattenburg

Proximity X-ray lithography (XRL), using wavelengths between 0.8 and 1.5 nm, provides a near-ideal match to the "system problem" of lithography for feature sizes from 500 to 30 nm, by virtue of "absorption without scattering" and recently developed mask technology. The effects of photoelectrons, at one time thought to be problematic, are now understood not to limit resolution. With experiments and simulations via Maxwell's equations, we show that useful resolution is not limited by diffraction until linewidths are below 50 nm. It is critically important to optimize the source spatial incoherence to eliminate the deleterious effects of high spatial frequencies. Mask architecture and patterning methods are presented which we believe are compatible with manufacturing at linewidths from 500 to 30 nm. Distortion due to mask frame flexing and absorber stress can now be eliminated. Elimination of distortion at the pattern generation stage remains the problem of greatest concern. We discuss a proposed method of spatial-phase-locked electron-beam lithography which could solve this problem.

Our new interferometric alignment scheme has achieved 18-nm alignment at  $3\sigma$ . We assert that projection XRL using multilayer mirrors at 13 nm can never match the present performance of proximity XRL. Applications of sub-100-nm XRL, including MOS, quantum-effect, and optoelectronic devices are discussed which illustrate the benefits of high resolution, process robustness, low distortion, low damage, and high throughput.

# Introduction

In comparison to other forms of radiation used in lithography (uv and deep-uv photons, electrons, ions) X-rays have the unique property that in their interaction with the material of the mask or the substrate, scattering is negligible. This is because in the wavelength range of interest for lithography (0.5–1.5 nm and 4.5 nm), the real part of the index of refraction is very close to unity. The imaginary part of the index, which corresponds to absorption, depends on atomic number, Z, and wavelength,  $\lambda$ . The essential challenge in creating an X-ray lithography technology [1] was to pick a wavelength such that high-Z absorbers such as gold had sufficient absorption (~90%) in thicknesses that could be

°Copyright 1993 by International Business Machines Corporation. Copying in printed form for private use is permitted without payment of royalty provided that (1) each reproduction is done without alteration and (2) the Journal reference and IBM copyright notice are included on the first page. The title and abstract, but no other portions, of this paper may be copied or distributed royalty free without further permission by computer-based and other information-service systems. Permission to republish any other portion of this paper must be obtained from the Editor.

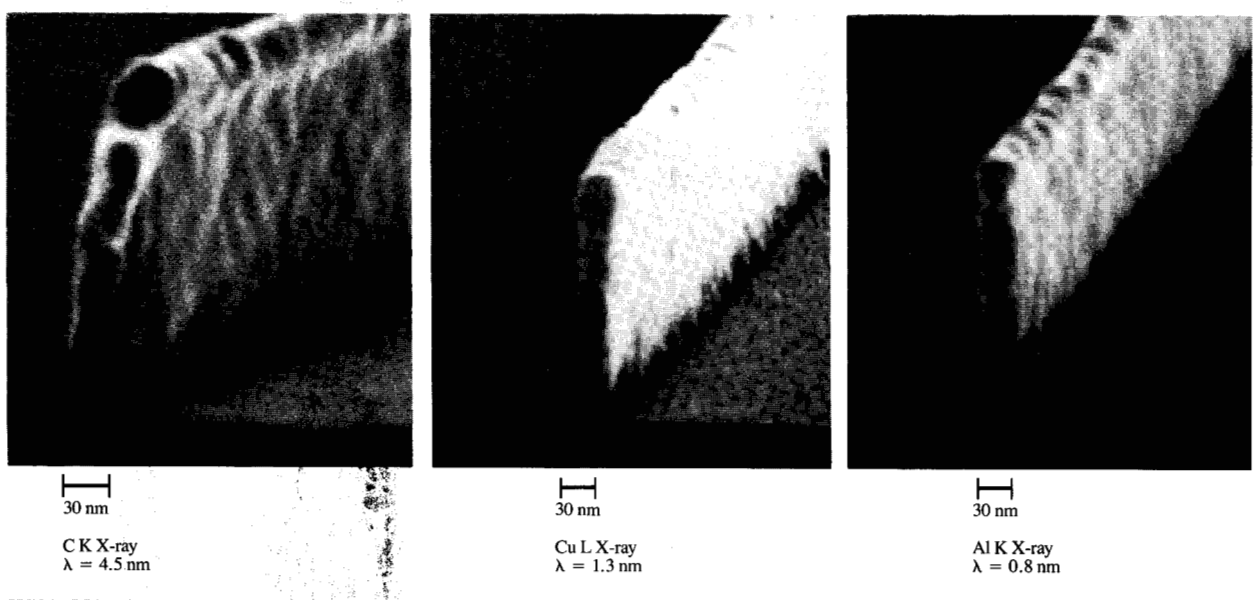


Figure 1

Using a mask with 30-nm-wide gold absorber stripes, 30-nm-wide PMMA resist structures, standing alone in an otherwise completely exposed field, are exposed and developed on a Si substrate using the three X-ray lines indicated. The results demonstrate the absence of proximity effects due to photoelectrons. (Micrograph by K. Early.)

conveniently patterned at the desired submicron dimensions, while at the same time a supporting membrane made of low-Z material could have sufficient stiffness to prevent pattern distortion, and still transmit more than about 50% of the incident X-ray flux. The first published reports on X-ray lithography [1-3] illustrated clearly the virtues of absorption without scattering. For example, optical defects on the mask were not printed with the X-rays, and the absorber pattern on the mask was replicated in thick resist with the highest fidelity, and in a pattern that had isolated features standing alone in an otherwise completely exposed field. The so-called proximity effects, common to e-beam lithography, were absent. It was these aspects (commonly referred to as process robustness and latitude) that gave X-ray lithography enormous promise in comparison to competitive parallel-exposure techniques and persuaded us to continue developing it vigorously. One can make a strong case that a lithography technique that provides absorption without scattering, and also low distortion, is ideally matched to the "system problem of lithography" [4].

In this paper we assert that by proper choice of operating wavelength, proper design of the mask, and optimization of the source spatial coherence, X-ray lithography is readily extendable to feature sizes of 100 nm at mask-substrate gaps of  $10-15 \mu m$ . We further show

that 50-nm lithography is feasible in a manufacturing-compatible configuration, and that it may even be possible to manufacture at 30-nm or even 20-nm feature sizes, although the latter will require a modification of the "gap paradigm."

#### Limits to resolution

Two factors limit resolution in X-ray lithography: photoelectron range and diffraction. We present the modern perspective on these two factors.

#### Photoelectrons

For many years it was assumed that the resolution of X-ray lithography was limited by the maximum range of the photo- and Auger electrons that are released when an X-ray photon is absorbed [1, 2, 5]. Experiments by Early et al. [6] and Deguchi et al. [7], and simulation by Murata et al. [8] clarified that this is not the case. The experimental results of Early et al. are shown in Figure 1. The 30-nm linewidths on the mask were faithfully replicated in PMMA resist at wavelengths of 4.5, 1.3, and 0.8 nm. The corresponding maximum photoelectron ranges are <5 nm, 20-30 nm, and 40-70 nm, respectively. Note that the pattern, an isolated, unexposed 30-nm-wide line of PMMA in an otherwise completely exposed field, is a geometry designed to maximize any deleterious "proximity" effects of photoelectrons. In order to

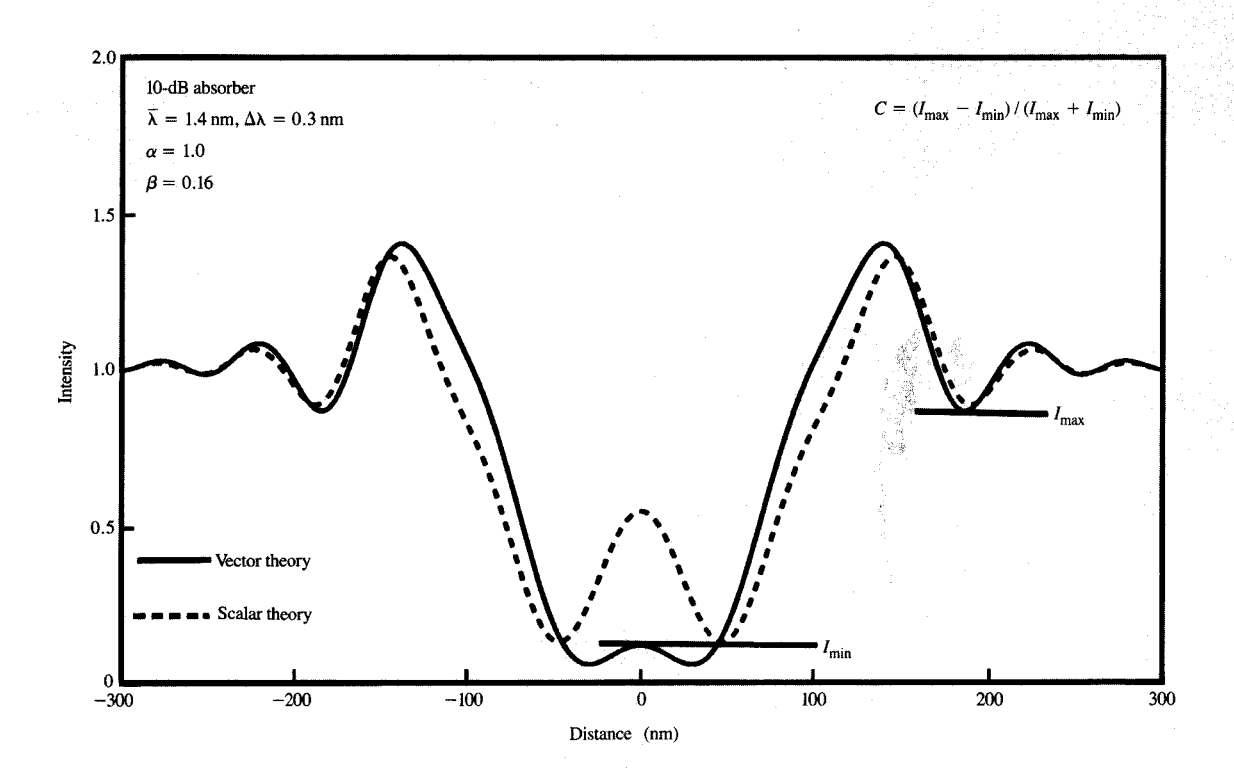


Figure 2

Plot of irradiance (intensity) as a function of position for a 100-nm-wide gold absorber (10 dB) at a gap corresponding to  $\alpha = 1$  for a Fe-plasma X-ray source. Note that the scalar theory predicts a middle stripe, whereas Maxwell's equations do not. Our definition of contrast, C, is also shown.

understand the results of Figure 1, one must consider not the maximum range of photoelectrons but, rather, the spatial distribution of energy deposited by electrons released after X-ray absorption. We call this the energy-deposition point-spread function (EDPSF). The EDPSF is dominated by the very short-range (~5 nm) Auger electrons, whose energy is characteristic of the resist materials, not the exciting photon. Photoelectrons contribute only a low-level background. One must convolve this EDPSF with the irradiance distribution in the X-ray image. When this is done, it becomes clear that feature sizes down to 20 nm are feasible using wavelengths of ~1 nm and longer.

Murata's simulation and results of Ogawa et al. [9] have shown that with wavelengths shorter than the Si K edge at 0.68 nm, considerable problems arise as a result of photoelectrons originating in the substrate and propagating back into the resist. Some synchrotron spectra include a significant amount of such harder X-rays, an obviously undesirable situation [10]. However, it is relatively easy to

eliminate such X-rays and operate a synchrotron in a more favorable wavelength range, e.g.,  $\lambda > 0.8$  nm.

#### • Diffraction

In 1989 B. J. Lin published a set of calculations predicting image degradation in X-ray replication of lines, spaces, contact cuts, and gratings [11]. He assumed plane-wave illumination and Kirchhoff-approximation boundary conditions; i.e., he assumed that immediately downstream from the mask the transmitted field at the edge of any feature makes an abrupt transition from maximum to minimum. Using this model he predicted very limited depth of focus and limited exposure latitude for X-ray lithography. It is now well known that Lin's model was spurious [12-16]. The collimated plane-wave illumination that Lin assumed is a worst-case condition, which gives rise to edge ringing [12-14], in much the same manner that collimated laser illumination degrades the performance of an optical microscope or stepper. In other words, the illumination should have some spatial incoherence. Also,

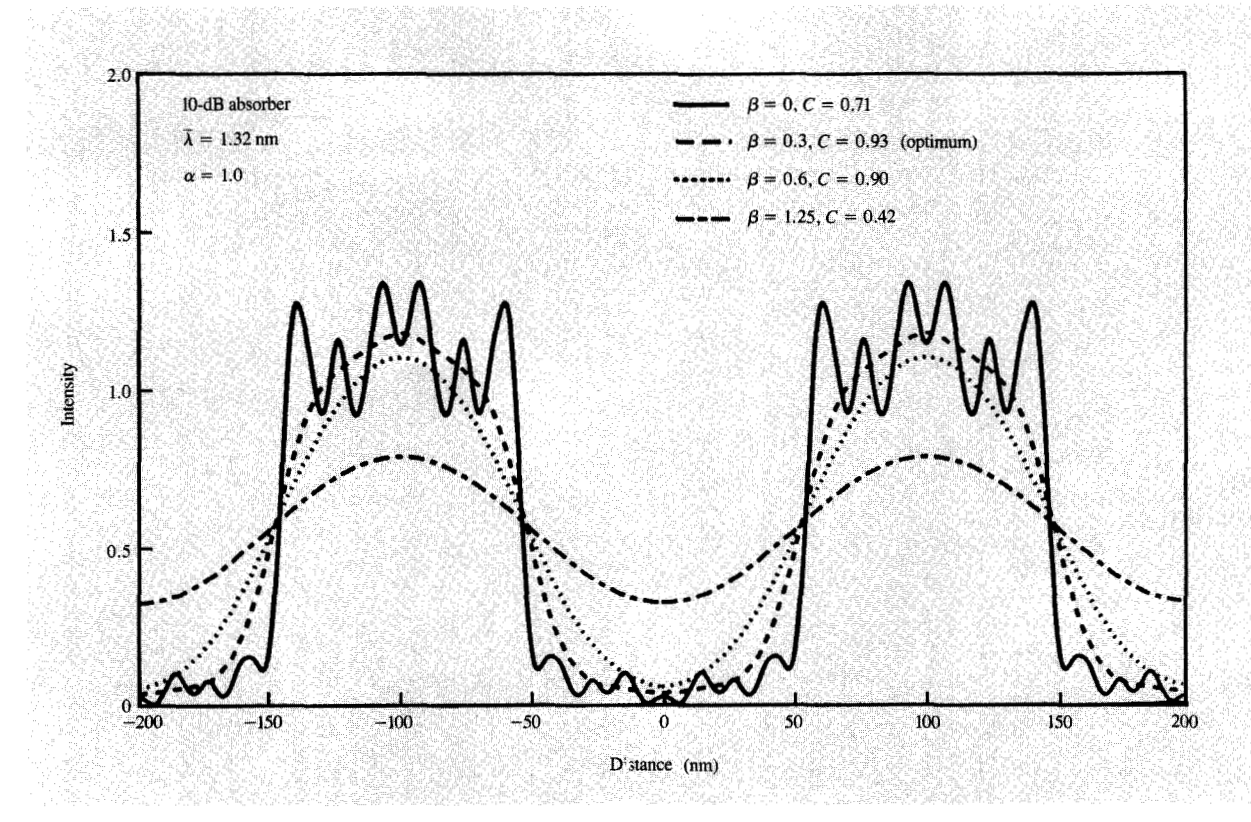


# Figure 3

Plots of intensity (irradiance) as a function of position for a 200-nm-period grating with 100-nm linewidth, 10-dB absorber, at a gap corresponding to  $\alpha=1$  (7.6  $\mu$ m for  $\lambda=1.32$  nm), for several values of penumbral blur. Note that ripple and edge ringing are eliminated by introducing some spatial incoherence, and that contrast increases as  $\beta$  is increased from 0 to 0.3, and then decreases.

an X-ray absorber is a lossy dielectric, hundreds of wavelengths thick, and cannot produce an abrupt transition in the field amplitude, as Lin assumed [15–17]. Moreover, the absorber introduces a phase shift.

Figure 2 illustrates the difference one obtains in the quality of the aerial image when a calculation based on Maxwell's equations and the real dielectric properties of the absorber is carried out [16]. Similar results have been obtained by others [17]. Figure 3 shows that edge ripples are absent when source spatial coherence is properly adjusted. In these figures,  $\beta$  is a parameter that indicates the "10% to 90%" penumbral edge blurring,  $\delta$ , due to the finite source size (i.e., spatial incoherence),

$$\beta = \delta/W_{\min}, \qquad (1)$$

where  $W_{\min}$  is the minimum linewidth. The parameter  $\alpha$  (reciprocal of the square of the so-called Fresnel number) indicates the mask-sample gap, G, via

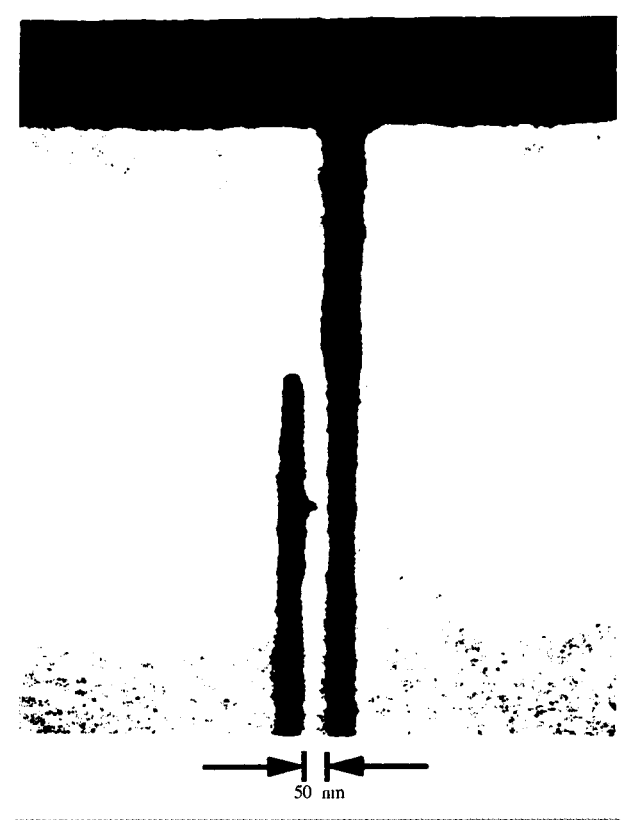
$$G = \alpha W_{\min}^2 / \lambda, \tag{2}$$

where  $\lambda$  is the source wavelength. Analysis and experiment [16–18] show that an  $\alpha$  value as large as 1.5 is tolerable if source spatial coherence is optimized; i.e.,  $\beta \sim 0.5$ . This corresponds to introducing a penumbral blur at each feature edge of about half the minimum linewidth. It is somewhat surprising that such a large penumbral blurring actually results in an improvement in image quality, but it makes sense when one realizes that by such blurring one is, in effect, suppressing spatial frequencies that are higher than the fundamental, thereby avoiding edge ringing, which can be problematic.

Figure 4 shows the X-ray replication of a pattern for a planar resonant-tunneling field-effect transistor (PRESTFET) having 50-nm lines and spaces. The gap was 2.72  $\mu$ m and the wavelength 1.32 nm (Cu L line radiation), corresponding to  $\alpha = 1.44$ . Penumbral blur was 19.6 nm, full width at half maximum; i.e.,  $\beta = 0.4$ . This result [18] was obtained over a broad exposure range (factor of 2.3), and is in accord with theoretical predictions [16]. The implication of this experimental result and additional

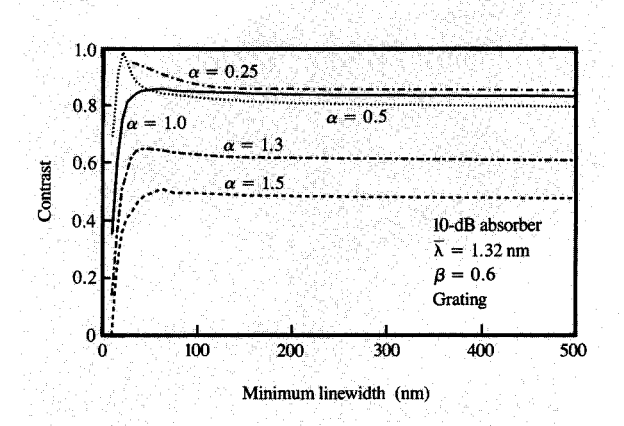
theoretical modeling is that 100-nm features can be replicated at 15- $\mu$ m gaps using 1-nm radiation if the source, as viewed from the substrate, subtends ~3.5 mrad.

Figure 5 plots image contrast (defined in Figure 2) versus minimum feature size for several values of  $\alpha$ , assuming appropriate penumbra [16]. For 50-nm features, a contrast of 0.5 is obtained at  $\alpha = 1.5$ , which corresponds to  $G = 2.8 \mu m$  at the assumed wavelength,  $\lambda = 1.32 \text{ nm}$ . If, instead,  $\lambda = 1$  nm, and if such wavelength scaling is valid,  $G = 3.8 \mu m$ . We routinely use such gaps, and even smaller gaps, in research [19]. Nevertheless, there is some skepticism that such gaps would be feasible in a future manufacturing implementation that required 50-nm features. Clearly, there is no difficulty making X-ray mask membranes that are optically flat [19]. This is a routine process in our laboratory. Substrates can be made optically flat by means of pin chucks or adaptive pin chucks, which have already been described [20]. The difficulty is not flatness but dust particles. These can be readily detected by light scattering prior to exposure.



## Figure 4

Scanning electron micrograph of a 100-nm-pitch (50-nm lines and spaces) interdigital electrode pattern exposed with a 1.32-nm X-ray (Cu L) at a mask-substrate gap of 2.72  $\mu$ m and a penumbral blur of 19.6 nm FWHM ( $\alpha=1.44$ ;  $\beta=0.4$ ). This implies that 100-nm features can be replicated at  $G=15~\mu$ m with  $\lambda=1$  nm. (Micrograph by W. Chu.)



# Figure 5

Plots of contrast versus minimum linewidth for five values of  $\alpha$  (the parameterized gap),  $\beta=0.6$ , and  $\lambda=1.32$  nm. Note that the actual gap varies with linewidth W as  $G=\alpha W^2/\lambda$ .

However, methods for their selective removal are not well developed. This does not seem to be a fundamental or even a difficult problem. For example, in our lab we have used a hypodermic needle connected to a vacuum hose as a "micro-vacuum cleaner" to remove individual dust particles. Bombardment and removal of dust with CO<sub>2</sub> or Ar "snow" which then fully volatilizes has been described [21].

At 30-nm features the calculated maximum gap is  $1.3~\mu m$ , and one is forced to contemplate contact between mask and substrate. This is also done routinely in our lab without damage to either mask or substrate. The fear of contact, a leftover from the days of contact printing on Si wafers with stiff glass masks, is not well founded because X-ray mask membranes are readily deflected, not damaged, by dust particles or other surface asperities. Whether contact, to achieve sub-30-nm features, would ever be feasible in manufacturing remains to be determined, but cannot be ruled out in advance. The atomic force microscope is testimony that our intuitions with regard to substrate damage are not always accurate.

# Mask configuration for $\lambda > 1$ nm

Figure 6 shows a mask configuration suitable for the 1.32-nm radiation that we have used for nanolithography. At a wavelength of 1 nm, the Au and W thicknesses would need to be increased to 360 and 500 nm, respectively, to provide 10-dB attenuation. The mask of Figure 6 is suitable also for the Fe spectrum of a laser-produced plasma (mean  $\lambda = 1.4$  nm). Human intuition would suppose that a membrane thickness of 1  $\mu$ m is too weak

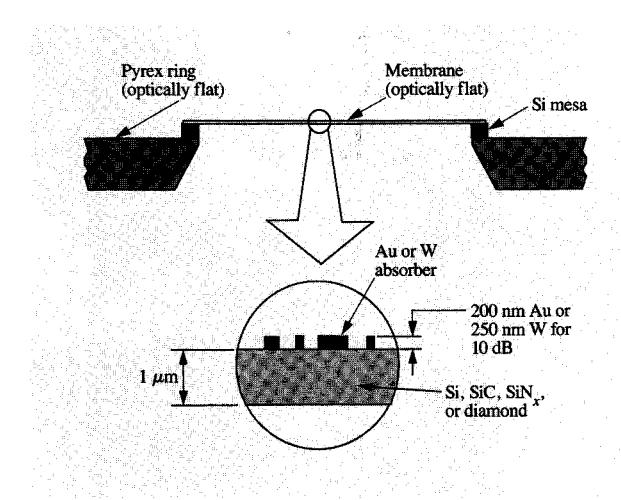


#### Figure 6

X-ray mask configuration for  $\lambda=1.32$  nm; suitable for lithography from 1000-nm to below 50-nm feature sizes. The mask membrane is typically flatter than 0.25  $\mu$ m, allowing gaps below 5  $\mu$ m.

and fragile for practical applications, but this is not the case. We regularly ship such masks by ordinary mail in conventional wafer containers, and we routinely use 1.7- $\mu$ m-thick Si-rich SiN $_x$  membranes of 20 mm diameter as vacuum windows!

The primary concern in any mask technology is distortion, either random or uncontrolled. In X-ray lithography this can arise from four sources: the original mask patterning; distortion of the Pyrex mask frame; distortion induced by radiation damage, or distortion induced by absorber stress. The first is discussed in the next section. The second is a mechanical fixturing problem and is presumably solvable either by kinematic mounting or by making the frame sufficiently sturdy. Membranes of SiC and single-crystal Si are unaffected by large doses of X radiation corresponding to over 10<sup>6</sup> exposures [22]. A fully radiation-stable SiN<sub>x</sub> has yet to be developed. Distortion induced by absorber stress can be eliminated by reducing absorber stress. Fortunately, the means for doing this are reasonably well understood.

As a rule of thumb, distortion at any point in a pattern should not exceed 1/5 to 1/10 of the minimum feature size. For optoelectronic devices, distortion tolerances might be considerably tighter than this (i.e., long-range spatial coherence is required). In the case of sputtered W absorber, intrinsic stress depends on the pressure during deposition, which can be readily monitored and controlled [23–25]. In a dedicated system, stresses below  $5 \times 10^7$  dyn/cm<sup>2</sup> (5 MPa) have been consistently achieved [24–27]. **Figure 7** shows that a stress of this level in a

 $100 \times 100$ - $\mu$ m W pad (10-dB attenuation) located off-center on a 31-mm-diameter Si<sub>3</sub>N<sub>4</sub> membrane, 1  $\mu$ m thick (our current standard), causes only 0.25 nm distortion, which is negligible for all conceivable applications. For the types of patterns encountered in practical applications, in which absorber is more uniformly distributed over the membrane, distortion would be even less than indicated in Figure 7. With W, a stress level of 10 MPa or less can probably be achieved routinely in a mass production environment. Clearly, SiC and diamond membranes, although stiffer than SiN<sub>x</sub>, are not essential in order to achieve zero distortion. SiC has an advantage over SiN<sub>x</sub> in that it can be a semiconductor and is radiation-stable. The same is true of crystalline Si.

In the case of electroplated gold absorber, stress depends on plating current density. By proper design of the plating fixtures, a stress of 10 MPa or less is achievable [28]. However, a problem with Au is that temperature cycling, as encountered, for example, in resist stripping, causes the stress to change [29]. Further research is needed on this issue.

Thus, it would appear that masks compatible with the 1.3-nm wavelength, having membrane thickness  $\sim 1~\mu\text{m}$ , absorber thickness  $\sim 0.25~\mu\text{m}$ , and diameters of 30-40~mm, are sufficiently rugged and free of distortion for use in manufacturing. It is noteworthy that these masks are applicable not just to 0.5- or 0.25- $\mu$ m features, but to sub-100-nm and even sub-50-nm regimes as well.

#### Mask patterning

At MIT we pattern X-ray masks using a variety of techniques: e-beam lithography, photolithography, holographic lithography, X-ray lithography (i.e., mask replication), and ion-beam lithography. The e-beam work is done outside, either at the IBM Thomas J. Watson Research Center [30] or at the Naval Research Laboratory (NRL). It is noteworthy that our gold plating base is relatively thin (5 nm NiCr, 10 nm Au) in order to minimize proximity effects due to electron backscattering. (If pinholes are a concern, one could use a thicker plating base of Ni coated with only a very thin film of Au.) In fact, a large fraction of the incident 50-keV electrons pass entirely through the mask membrane, further reducing the electron backscattering. An adhesion promoter is used between the resist (typically PMMA) and the gold plating base. Once features are developed, the adhesion promoter is removed by a brief immersion in an oxygen plasma or a quick dip in a dilute HF solution, and electroplating is commenced. We use two types of plating solution, BDT-510<sup>2</sup> and Technigold-25E.<sup>3</sup> When very tall lines (i.e., height-to-width ratio >4) are plated, we keep the

<sup>1</sup> MicroSi MS-805 Adhesion Promoter solution for noble metal substrates, Huls

America, Bristol, PA.

<sup>2</sup> Sel-Rex BDT-510 Plating Solution, OMI International Corp., Nutley, NJ.

<sup>&</sup>lt;sup>3</sup> Technigold 25E, Technic, Inc., Cranston, RI.

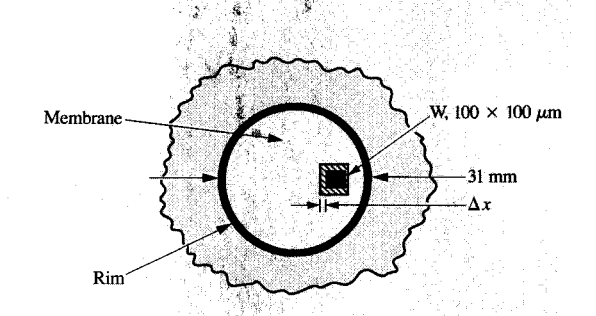
substrates immersed in fluid to prevent surface tension from exerting a force on the fine resist features [28, 31]. That is, the substrate is never allowed to dry until after the plating is completed. Development is quenched in alcohol and then water; the HF etch is quenched in water, but the resist is never uncovered by fluid.

A serious problem associated with e-beam patterning is pattern placement accuracy. This problem arises because of distortion within an e-beam scan field, and because of errors in stitching fields together. There are many causes of the latter error. In brief, the problem arises because "the loop is not closed." That is, the e-beam system's laser interferometer and its associated computer keep track of the stage position, but not the position of the electron beam. The beam can drift with respect to its assumed location as a result of charging, thermal expansion, and a multitude of other causes. Our proposal to overcome this difficulty is to place a holographically generated global fiducial grid on the X-ray mask membrane itself, thereby closing the loop by keeping track of the beam position relative to the fiducial grid [32]. We call this proposal "spatial-phase-locked e-beam lithography" (SPLEBL) and are currently trying to implement it in collaboration with D. Kern and S. Rishton at the IBM Thomas J. Watson Research Center [33]. It is important to emphasize that with SPLEBL one never looks at an individual unit cell of the grid but instead takes advantage of the perfect, longrange, coherent periodicity of the grid and employs signal processing methods not unlike those upon which the lockin amplifier is based. As a result, extremely high-fidelity e-beam lithography is anticipated. The global grid also allows one to correct distortion within a scan field [34]. The (SPLEBL) scheme would also work well with scanning ion beam lithography, which also suffers from the "open-loop problem."

Once a master mask is made by e-beam lithography, or any other technique, or combination of techniques, replica masks are readily made. This is the strategy we generally follow and suggest that it would be preferred in a manufacturing setting. That is, the master masks could be made using electroplated gold absorber and, after inspection, repair, and production of replicas, they could be stored at a controlled temperature to avoid any changes in the gold stress [29]. Replicas could have their absorber patterns formed by dry etching rather than electroplating, and could use tungsten for better stability and stress control [22–26].

#### Mask alignment

It has been known for many years that misalignment between mask and substrate of the order of 10 nm is readily detected by optical means, especially by grating-based interferometric schemes [35–39]. Ishihara et al. demonstrated a misalignment detectivity of ~5 nm [37].



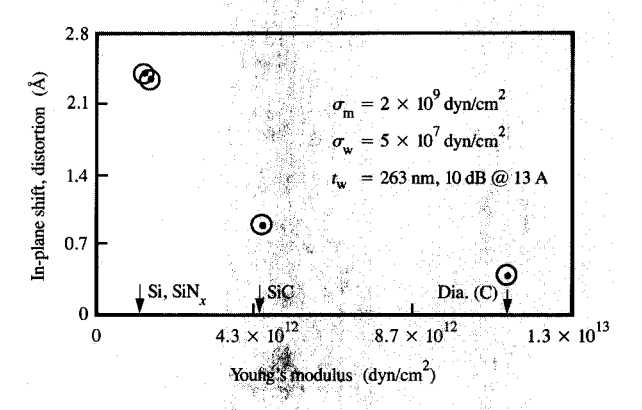


#### Figure 7

In-plane distortion for a worst-case condition of a large (100  $\times$  100  $\mu \rm m)$  off-center pad, calculated using a finite-element analysis program. A W thickness sufficient to give 10-dB attenuation and a tensile stress of 5  $\times$  10 $^7$  dyn/cm $^2$  are assumed. For all membrane types (Si, SiN<sub>x</sub>, SiC, and diamond) the distortion is below 1 nm. ( $\sigma_{\rm m}$  is membrane stress,  $\sigma_{\rm w}$  is W metal stress, and  $t_{\rm w}$  is metal thickness.)

However, such interferometric schemes have not demonstrated  $3\sigma$  alignments close to their detectivity, presumably because of the nonideal signals obtained when realistic manufacturing conditions are employed [39]. To circumvent the shortcomings of previous interferometric schemes, we have investigated an approach which combines the high sensitivity to lateral displacement that is characteristic of dual-grating interferometry with the best features of schemes that form dark-field images of proximity alignment marks. A detectivity of 3.5 nm and a  $3\sigma$  alignment of 18 nm have been demonstrated in a controlled set of experiments [40, 41]. Our current objective is to achieve a working  $3\sigma$  alignment below 10 nm, entirely under computer control, and to integrate the new system with a laser-plasma X-ray source from Hampshire Instruments. In comparison to so-called global

<sup>&</sup>lt;sup>4</sup> Hampshire Instruments, Inc., Rochester, NY.

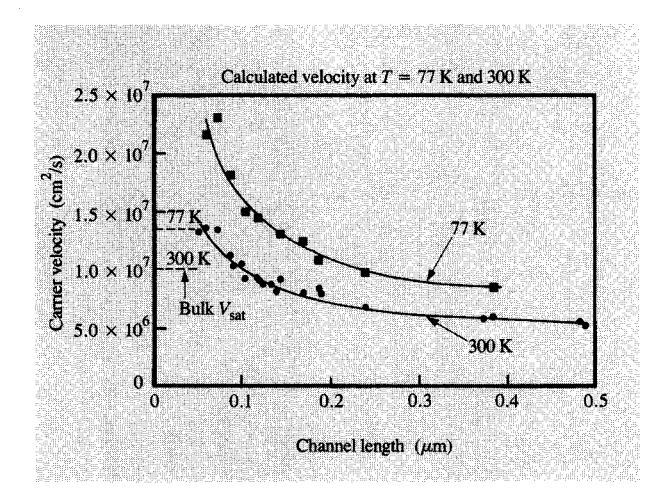


# Figure 8

Plot of effective carrier velocity in NMOS transistors versus channel length, at 300 K and 77 K. Dotted lines indicate the corresponding bulk carrier velocities.

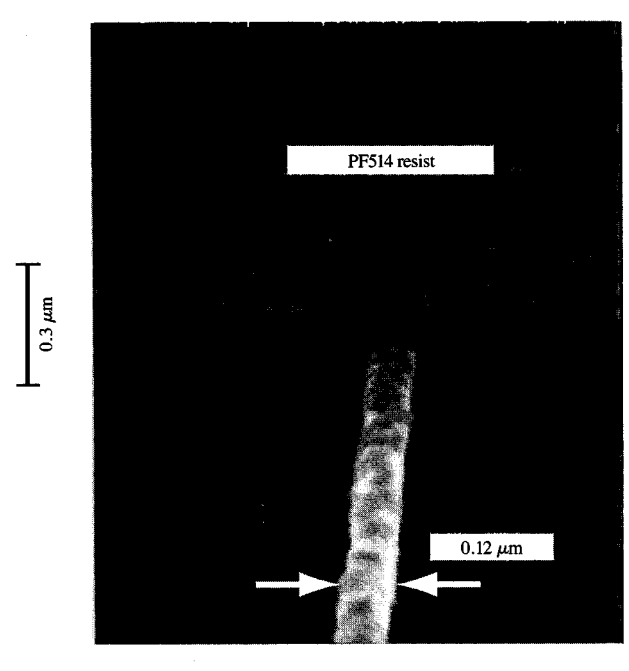


# Figure 9

Gate pattern for a 0.1- $\mu$ m-channel-length MOSFET exposed in high-speed X-ray resist using  $\lambda=1.32$  nm and a gap of several  $\mu$ m. (Micrograph by H. Hu.)

alignment schemes, which use laser interferometry to keep track of alignment stage position, there are significant advantages to (and manifest simplicity in) a scheme in which mask and wafer are held in close proximity and alignment is achieved by interferometrically referencing an alignment mark on one member to an alignment mark on the other at each exposure location.

# impact of X-ray nanolithography

To date, X-ray lithography has been used to fabricate sub-100-nm-feature devices only in academic research. However, the results obtained and the new technologies developed indicate that manufacturing in the nanolithography domain should be feasible, at least down to 50 nm and perhaps beyond. We discuss here a few areas where the high resolution, high throughput, process robustness, and low distortion of X-ray lithography will likely prove crucial.

Figure 8 shows the effective carrier velocity in a series of non-self-aligned Si NMOS devices, differing in channel length, but all made on the same substrate by X-ray nanolithography [42]. These were the first devices that showed velocity overshoot at 77 K and room temperature. (Earlier, Chou had seen velocity overshoot at 4 K, also on X-ray fabricated devices [43].) They also showed intrinsic transconductance above 1 S/mm, and reduction of hotelectron effects at channel lengths below 150 nm [44]. It is now generally agreed that high-density 100-nm CMOS circuits appear feasible. X-ray lithography provides the only cost-effective means of manufacturing them. Some of the novel technologies described here will almost certainly have to be employed. Figure 9 is a micrograph of the gate pattern for a 100-nm-channel-length MOSFET exposed in a high-speed, chemically amplified resist (PF-514) by X-ray lithography.

A wide variety of quantum-effect devices and structures have been fabricated using X-ray nanolithography, including lateral-surface superlattices [45–49], quantum-wire arrays [50], and electron waveguides [51]. In general, they exhibit quantum effects that are sharper and more robust than in devices made by direct-write e-beam lithography. In the waveguides, for example, sharp quantized conductance steps were observed at 750 nm length and beyond [51], presumably due to the absence of radiation-induced damage.

Optoelectronic systems of the future will include a variety of fine-period structures for distributed feedback (DFB) lasers, channel-dropping filters [52], and similar components. In addition to possessing periods of ~100-200 nm, patterns will have to be spatially coherent over areas that are tens to hundreds of micrometers across. At the present time, e-beam lithography systems are incapable of writing such spatially coherent patterns. The proposed spatial-phase-locked e-beam lithography [32, 33], described above, should be able to solve this problem. Figure 7 implies that if the patterns are created with sufficient spatial coherence on X-ray mask membranes, they can be replicated over large substrate areas without additional distortion.

# **Projection X-ray lithography**

It is widely assumed in the trade literature [53] that soft X-ray projection lithography (SXPL) using multilayer reflectors will replace proximity X-ray lithography (PXRL), for the same reason that optical projection lithography replaced proximity printing in IC manufacturing. However, in technology such analogies sometimes do not hold: The nuclear submarine replaced the fossil-fueled submarine, but the nuclear aircraft has not displaced the fossil-fueled jet!

SXPL will not be able to match the lithographic quality of PXRL (i.e., vertical profiles in single-layer-thick resist and over topography) unless the operating wavelength is shifted down from the current 13 nm to at least 4.5 nm, the carbon edge. This is because the absorption of 13-nm radiation in resist is too high. However, the theoretical maximum efficiency of multilayer mirrors at 4.5 nm is only 10%. Moreover, for diffraction-limited operation the surfaces of the several (four to seven) mirrors required by a projection system would have to follow the design curvature, which is aspheric, to within  $\lambda/(8\sqrt{n})$ , where n is the number of mirrors. Assuming n = 4, this corresponds to an allowed deviation of 0.8 nm for  $\lambda = 13$  nm, and 0.3 nm for  $\lambda = 4.5$  nm! Such tolerances would have to be held during exposure, despite each mirror absorbing 40% or more of the incident radiation in a vacuum environment. A reflection reduction projection system cannot, even in principle, achieve as low a distortion as predicted in Figure 7.

The driving force for the development of SXPL appears to be the presumptions that one-to-one X-ray masks cannot be fabricated with sufficient overlay precision, and that the gaps required by PXRL (15  $\mu$ m at 100-nm linewidths; 3.8  $\mu$ m at 50-nm features) will not be allowed in manufacturing. These presumptions are highly questionable at best. A one-to-one projection system based on arrays of zone plates, operated at  $\lambda = 1$  or 4.5 nm, does, however, appear to be feasible [54, 55].

# **Conclusions**

A unique feature of X-rays, absorption without scattering, makes them especially well suited to the system problem of lithography. Clearly, the lithography quality, as indicated in resist profiles, is superb, from micrometer linewidths to perhaps 20 nm [6]. Concerns about resolution limitations due to photoelectrons have turned out to be unfounded, at least for  $\lambda > 0.8$  nm. A more careful analysis of near-field diffraction using Maxwell's equations and employing partially incoherent illumination has revealed that mask–sample gaps can be about three times larger than previously believed; i.e.,  $\alpha = 1.5$  in Equation (2). Mask technology for the 1.3-nm wavelength has progressed to the point where pattern placement error in the e-beam lithography remains the major problem to

solve. Spatial-phase locking via a global fiducial grid on the membrane is proposed as a solution. A  $3\sigma$  alignment of 18 nm has been demonstrated in a laboratory system that combines the best features of interferometric and imaging schemes. Research on devices with 100-nm and sub-100-nm features, fabricated by X-ray lithography, has pointed the way toward manufacturing in this regime. The full power of X-ray lithography may well be essential for manufacturing future optoelectronic systems, which require spatial fidelity well beyond what is required for ICs.

# **Acknowledgments**

This work was supported by the Joint Services Electronics Program (DAAL03-92-C-0001), the National Science Foundation (ECS 9016437), NASA (NAS8-36748), and DARPA through the Department of the Navy (N00019-92-K-0021). The authors are grateful to the many students and staff members at MIT who have contributed to the developments described here.

### References

- D. L. Spears and H. I. Smith, "High-Resolution Pattern Replication using Soft X-Rays," *Electron. Lett.* 8, 102-104 (1972).
- D. L. Spears, H. I. Smith, and E. Stern, "X-Ray Replication of Scanning Electron Microscopy Generated Patterns," Proceedings of the 5th International Conference, Electron and Ion Beam Science and Technology, Houston, TX, May 7-11, 1972, R. Bakish, Ed., The Electrochemical Society, Inc., Princeton, NJ, 1972, pp. 80-91.
- 3. H. I. Smith, D. L. Spears, and S. E. Bernacki, "X-Ray Lithography: A Complementary Technique to Electron Beam Lithography," J. Vac. Sci. Technol. 10, 913-917 (1973).
- 4. H. I. Smith and M. L. Schattenburg, "Why Bother with X-Ray Lithography?" Proc. SPIE 1671, 282-298 (1992).
- R. Feder, E. Spiller, and J. Topalian, "Replication of 0.1 μm Geometries with X-Ray Lithography," J. Vac. Sci. Technol. 12, 1332-1334 (1975).
- K. Early, M. L. Schattenburg, and H. I. Smith, "Absence of Resolution Degradation in X-Ray Lithography for λ from 4.5 nm to 0.83 nm," *Microelectron. Eng.* 11, 317-321 (1990); K. R. Early, Ph.D. thesis, Massachusetts Institute of Technology, August 1991, *Technical Report No.* 565, MIT, RLE, Cambridge, MA.
- K. Deguchi, T. Ishiyama, T. Horiuchi, and A. Yoshikawa, "Effects of Photo- and Auger Electron Scattering on Resolution and Linewidth Control in SR Lithography," JJAP Series 4, Proceedings of the Third International MicroProcess Conference, MPC-90, 1990, pp. 100-104.
- K. Murata, "Theoretical Studies of the Electron Scattering Effect on Developed Pattern Profiles in X-Ray Lithography," J. Appl. Phys. 57, 575-580 (1985); K. Murata, M. Tanaka, and H. Kawata, "Theoretical Study of Energy Absorption on X-Ray Lithography with Monochromatic X-Rays," Optik 84, 163-168 (1990).
   T. Ogawa, K. Mochiji, Y. Soda, and T. Kimura, "The
- T. Ogawa, K. Mochiji, Y. Soda, and T. Kimura, "The Effects of Secondary Electrons from a Silicon Substrate on SR X-Ray Lithography," JJAP Series 3, Proceedings of the 1989 International Symposium on MicroProcess Conference, 1989, pp. 120-123.

- M. L. Schattenburg and H. I. Smith, "X-ray Nanolithography—the Clearest Path to 0.1 and Sub-0.1 μm ULSI," JJAP Series 5, Proceedings of the 1991 International MicroProcess Conference, 1991, pp. 63-70.
- B. J. Lin, "Comparison of Projection and Proximity Printings—From UV to X-Ray," *Microelectron. Eng.* 11, 137 (1990); B. J. Lin, *Proc. SPIE* 1263, 80 (1990).
- H. K. Oertel, M. Weiss, H. L. Huber, Y. Vladimirsky, and J. R. Maldonado, "Modeling of Illumination Effects or Resist Profiles in X-Ray Lithography," Proc. SPIE 1465, 244 (1991).
- J. Z. Y. Guo and F. Cerrina, "Verification of Partially Coherent Light Diffraction Models in X-Ray Lithography," J. Vac. Sci. Technol. B 9, 3207 (1991).
- F. Cerrina and J. Z. Y. Guo, "Optimization of Partially Coherent Illumination in X-Ray Lithography," *Proc. SPIE* 1671, 442-450 (1992).
- M. L. Schattenburg, K. Li, R. T. Shin, J. A. Kong, and H. I. Smith, "Electromagnetic Calculation of Soft-X-Ray Diffraction from 0.1 μm Gold Structures," J. Vac. Sci. Technol. B 9, 3232–3236 (1991).
- S. D. Hector, M. L. Schattenburg, E. H. Anderson, W. Chu, A. Yen, and H. I. Smith, "Modeling and Experimental Verification of Illumination and Diffraction Effects on Image Quality in X-Ray Lithography," J. Vac. Sci. Technol. B 10, 3164 (1992).
- J. Z. Y. Guo, F. Cerrina, E. Difabrizio, L. Luciani, and M. Gentili, "Experimental and Theoretical Study of Image Bias in X-Ray Lithography," J. Vac. Sci. Technol. B 10, 3150 (1992).
- W. Chu, H. I. Smith, and M. L. Schattenburg, "Replication of 50 nm Linewidth Device Patterns Using Proximity X-Ray Lithography at Large Gaps," Appl. Phys. Lett. 59, 1641-1643 (1991).
- M. L. Schattenburg, K. Early, Y. C. Ku, W. Chu, M. I. Shepard, S. C. The, H. I. Smith, D. W. Peters, R. D. Frankel, D. R. Kelly, and J. P. Drumheller, "Fabrication and Testing of 0.1 μm-Linewidth Microgap X-Ray Masks," J. Vac. Sci. Technol. B 8, 1604-1608 (1990).
- M. Taniguchi, R. Funatsu, A. Inagaki, K. Okamoto, Y. Kenbo, Y. Kato, and I. Ochiai, "X-Ray Exposure System with Plasma Source for Microlithography," *Proc. SPIE* 1089, 240 (1989).
- R. Sherman, J. Grob, and W. Whitlock, "Dry Surface Cleaning Using CO<sub>2</sub> Snow," J. Vac. Sci. Technol. B 9, 1970-1977 (1991).
- Y. C. Ku, H. I. Smith, and I. Plotnik, "Low Stress Tungsten Absorber for X-Ray Masks," *Microelectron*. Eng. 11, 303-308 (1990).
- A. M. Haghiri Gosnet, F. R. Ladan, C. Mayeux, H. Launois, and M. C. Joncour, "Stress and Microstructure in Tungsten Sputtered Thin Films," J. Vac. Sci. Technol. B 7, 2663 (1989).
- Y. C. Ku, Lee-Peng Ng, R. Carpenter, K. Lu, H. I. Smith, L. E. Haas, and I. Plotnik, "In-Situ Stress Monitoring and Deposition of Zero Stress W for X-Ray Masks," J. Vac. Sci. Technol. B 9, 3297-3300 (1991).
- R. R. Kola, G. K. Celler, J. Frackoviak, C. W. Jurgensen, and L. E. Trimble, "Stable Low-Stress Tungsten Absorber Technology for Sub-Half-Micron X-Ray Lithography," J. Vac. Sci. Technol. B 6, 3301-3305 (1991).
- Y. C. Ku, M. H. Lim, J. M. Carter, and H. I. Smith, "Correlation of In-Plane and Out-of-Plane Distortion in X-Ray Lithography Masks," J. Vac. Sci. Technol. B 10, 3169 (1992).
- G. K. Celler, C. Biddick, J. Frackoviak, C. W. Jurgensen, R. R. Kola, A. E. Novembre, D. M. Tennant, and L. E. Trimble, "X-Ray Lithography with a Point Source Stepper," J. Vac. Sci. Technol. B 10, 3186 (1992).

- W. Chu, M. L. Schattenburg, and H. I. Smith, "Low-Stress Gold Electroplating for X-Ray Masks," Microelectron. Eng. 17, 223-226 (1992).
- W. A. Johnson, R. E. Acosta, B. S. Berry, and W. C. Pritchet, "Stress Reduction of Gold Absorber Patterns on X-Ray Masks," J. Vac. Sci. Technol. B 10, 3155 (1992).
- W. Chu, H. I. Smith, S. A. Rishton, D. P. Kern, and M. L. Schattenburg, "Fabrication of 50 nm Line-and-Space X-Ray Masks in Thick Au Using a 50 keV Electron Beam System," J. Vac. Sci. Technol. B 10, 118-121 (1992).
- H. I. Smith, E. H. Anderson, A. M. Hawryluk, and M. L. Schattenburg, "Planar Techniques for Fabricating X-Ray Diffraction Gratings and Zone Plates," Springer Series on Optical Sciences, X-Ray Microscopy, D. Rudolph and G. Schmahl, Eds., Springer-Verlag, Berlin, 1984, Vol. 43, pp. 51-61
- H. I. Smith, S. D. Hector, M. L. Schattenburg, and E. H. Anderson, "A New Approach to High Fidelity E-Beam Lithography Based on an In-Situ, Global Fiducial Grid," J. Vac. Sci. Technol. B 9, 2992-2995 (1991).
- 33. Juan Ferrera, Vincent V. Wong, S. Rishton, V. Boegli, E. H. Anderson, D. P. Kern, and H. I. Smith, "Spatial-Phase-Locked Electron-Beam Lithography for Fabricating X-Ray Masks for Optoelectronic Devices," to be presented at the 37th International Symposium on Electron, Ion and Photon Beams, San Diego, CA, June 1-4, 1993.
- E. H. Anderson, V. Boegli, M. L. Schattenburg, D. P. Kern, and H. I. Smith, "Metrology of Electron Beam Lithography Systems Using Holographically Produced Reference Samples," J. Vac. Sci. Technol. B 9, 3606-3611 (1991).
- D. C. Flanders, H. I. Smith, and S. Austin, "A New Interferometric Alignment Technique," Appl. Phys. Lett. 31, 426-428 (1977).
- J. Itoh and T. Kanayama, "Optical Heterodyne Detection of Mask-to-Wafer Displacement for Fine Alignment," Jpn. J. Appl. Phys. 25, L684-L686 (1986).
- S. Ishihara, M. Kanai, A. Une, and M. Suzuki, "A Vertical Stepper for Synchrotron X-Ray Lithography," J. Vac. Sci. Technol. B 6, 1652-1656 (1989).
- G. Chen, J. Wallace, F. Cerrina, S. Palmer, B. Newell, and J. Randall, "Experimental Evaluation of the Two-State Alignment System," J. Vac. Sci. Technol. B 6, 3222-3226 (1991).
- 39. K. Deguchi, K. Miyuoshi, H. Ban, H. Kyuragi, S. Konaka, and T. Matsuda, "Application of X-Ray Lithography with a Single-Layer Resist Process to Sub-Quartermicron Large-Scale Integrated Circuit Fabrication," J. Vac. Sci. Technol. B 10, 3145 (1992).
- 40. A. Moel Modiano, "An Aligner for X-Ray Nanolithography," Ph.D. Thesis, Massachusetts Institute of Technology, Cambridge, October 1992.
- 41. A. Moel Modiano, R. Frankel, J. Munroe, E. Moon, and H. I. Smith, "A Novel Moiré-Phase-Matching Alignment Technique with 6 nm-Sigma Precision," to be presented at the 37th International Symposium on Electron, Ion and Photon Beams, San Diego, CA, June 1-4, 1993.
- G. G. Shahidi, D. A. Antoniadis, and H. I. Smith, "Electron Velocity Overshoot in Sub-100 nm Channel Length MOSFETs at 77K and 300K," J. Vac. Sci. Technol. B 6, 137 (1988).
- S. Y. Chou, D. A. Antoniadis, and H. I. Smith, "Observation of Electron Velocity Overshoot in Sub-100nm-Channel MOSFETs in Si," *IEEE Electron Device Lett.* EDL-6, 665 (1985).
- G. G. Shahidi, D. A. Antoniadis, and H. I. Smith, "Reduction of Channel-Hot-Electron-Generated Substrate Current in Sub-150-nm Channel Length Si MOSFET's," IEEE Electron Device Lett. EDL-9, 497 (1988).

- K. Ismail, W. Chu, A. Yen, D. A. Antoniadis, and H. I. Smith, "Negative Transconductance and Negative Differential Resistance in a Grid-Gate Modulation-Doped Field-Effect Transistor." Appl. Phys. Lett. 54, 460 (1989)
- Field-Effect Transistor," Appl. Phys. Lett. 54, 460 (1989).
  46. K. Ismail, T. P. Smith III, W. T. Masselink, and H. I. Smith, "Magnetic Flux Commensurability in Coupled Quantum Dots," Appl. Phys. Lett. 55, 276 (1989).
  47. A. Toriumi, K. Ismail, M. Burkhardt, D. A. Antoniadis,
- A. Toriumi, K. Ismail, M. Burkhardt, D. A. Antoniadis, and H. I. Smith, "Resonant Magneto-Capacitance in a Two-Dimensional Lateral-Surface Superlattice," *Phys. Rev. B* 41, 12346-12349 (1990).
- Y. Zhao, D. C. Tsui, M. Santos, M. Shayegan, R. A. Ghanbari, D. A. Antoniadis, and H. I. Smith, "Magneto-Optical Absorption in a Two-Dimensional Electron Grid," Appl. Phys. Lett. 12, 1510-1512 (1992).
- K. Ismail, P. F. Bagwell, T. P. Orlando, D. A. Antoniadis, and H. I. Smith, "Quantum Phenomena in Field-Effect-Controlled Semiconductor Nanostructures," *Proc. IEEE* 79, 1106-1116 (1991).
- K. Ismail, D. A. Antoniadis, and H. I. Smith, "One-Dimensional Subbands and Mobility Modulation in GaAs/AlGaAs Quantum Wires," Appl. Phys. Lett. 54, 1130 (1989).
- W. Chu, C. C. Eugster, A. Moel, E. E. Moon, J. A. del Alamo, H. I. Smith, M. L. Schattenburg, K. W. Rhee, M. C. Peckerar, and M. R. Melloch, "Conductance Quantization in a GaAs Electron Waveguide Device Fabricated by X-Ray Lithography," J. Vac. Sci. Technol. B 10, 2966 (1992).
- 52. H. A. Haus and Y. Lai, "Narrow-Band Optical Channel-Dropping Filter," J. Lightwave Technol. 10, 57-62 (1992).
- 53. D. L. White, J. E. Bjorkholm, J. Bokor, L. Eichner, R. R. Freeman, T. E. Jewell, W. M. Mansfield, A. A. MacDowell, L. H. Szeto, D. W. Taylor, D. M. Tennant, W. K. Waskiewicz, D. L. Windt, and O. R. Wood II, "Soft X-Ray Projection Lithography," Solid State Technol. 34, 37 (1991).
- 54. M. Feldman, "Projection X-Ray Lithography Using Arrays of Zone Plates," Proceedings of the Electrochemical Society in Patterning Science and Technology, Number 2, W. Greene, G. Hefferon, and L. White, Eds., Proceedings Vol. 92-6, 136-146 (1991).
- 55. Scott D. Hector and Henry I. Smith, "Soft-X-Ray Projection Lithography Using Two Arrays of Phase Zone Plates," presented at the Third OSA Topical Meeting on Soft-X-ray Projection Lithography, Monterey, CA, May 10-12, 1993.

Received October 5, 1992; accepted for publication November 23, 1992

Henry I. Smith Massachusetts Institute of Technology, Department of Electrical Engineering and Computer Science, 77 Massachusetts Avenue, Cambridge, Massachusetts 02139. Professor Smith holds the Joseph F. and Nancy P. Keithley Chair in Electrical Engineering at MIT. In recent years his research has emphasized nanofabrication, methods for preparing semiconductor-on-insulator films, electronic devices, quantum effects in sub-100-nm structures, and optoelectronic device fabrication. He and his co-workers are responsible for a number of innovations in submicrometer-structure technology and applications, including conformable photomask lithography, X-ray lithography, interferometric alignment, graphoepitaxy, subboundary entrainment, achromaticholographic lithography, sub-100-nm Si MOSFETs, and a variety of quantum-effect structures such as lateral-surface superlattices and planar-resonant-tunneling field-effect transistors in GaAs/AlGaAs. Prof. Smith is a member of the APS, AVS, MRS, and Sigma Xi. He is a Fellow of the IEEE and a member of the National Academy of Engineering.

Mark L. Schattenburg Massachusetts Institute of Technology Center for Space Research, 70 Vassar Street, Cambridge, Massachusetts 02139 (marks@space.mit.edu). Dr. Schattenburg studied physics, receiving a B.S. degree from the University of Hawaii in 1978 and a Ph.D. from MIT in 1984. Since 1984 he has worked at MIT as a research scientist in the Center for Space Research and also in the Submicron Structures Laboratory. He currently leads a group responsible for the fabrication of X-ray transmission gratings for the Advanced X-ray Astrophysics Facility (AXAF), slated for launch by NASA in 1998. His research interests include X-ray lithography, micro/nanofabrication technology, X-ray optics/instrumentation, and X-ray astronomy.